Journal of Applied Polymer Science

Effect of Plasma Duty Cycle on Silver Nanoparticles Loading of Cotton Fabrics for Durable Antibacterial Properties

Aissam Airoudj, Lydie Ploux, Vincent Roucoules
Institut de Science des Materiaux de Mulhouse, IS2M - C.N.R.S. - UMR 7361 – UHA, 15, Rue Jean Starcky, 68057 Mulhouse Cedex, France
Correspondence to: A. Airoudj (E-mail: aissam.airoudj@uha.fr)

ABSTRACT: A facile method for strongly anchoring silver nanoparticles (AgNPs) onto cotton fabrics was reported. It consists in loading AgNPs onto the cotton fiber preliminary coated with maleic anhydride plasma polymer layer. This results in hydrolyzis and ring opening of anhydride groups followed by electrovalent bonding of silver ions and reduction in $NaBH_4$. X-ray photoelectron spectroscopy (XPS), infrared spectroscopy, and scanning electron microscope (SEM) were used to analyze changes in the surface chemical composition and morphology of the plasma modified fibers. The presence of AgNPs was confirmed by UV–Visible spectroscopy and atomic force microscopy (AFM) images. Remarkably, varying plasma duty cycle for plasma polymer deposition allowed tailoring the amount of loaded AgNPs. The highest amount of AgNPs was obtained with the lowest duty cycle values. Qualitative tests showed that silver containing plasma modified cotton displays significant antibacterial activity. © 2014 Wiley Periodicals, Inc. J. Appl. Polym. Sci. **2015**, *132*, 41279.

KEYWORDS: biomaterials; coatings; functionalization of polymers; surfaces and interfaces; textiles

Received 22 May 2014; accepted 11 July 2014
DOI: 10.1002/app.41279

INTRODUCTION

Functionalization of textile materials aiming at improving their performance for different applications (antistatic, flame retardant, self-cleaning, insect-repellent…) has attracted much attention in recent years. At the same time, there has been increased interest in the loading of nanoparticles onto fibers because of their numerous potential applications that open up new possibilities for engineering advanced properties.[1–3] In particular, silver in its uncharged state (AgNPs) have been on the central concern because they show strong inhibitory and bactericidal effects as well as a broad spectrum of antibacterial activities when oxidized in their ionic form (Ag^+).[4–7] However, the immobilization of silver species at textile surface is a challenging for interdisciplinary research bordering between materials and surface science.

Previous studies indicated that pretreatment of textiles by plasma process can improve loading of nanoparticles.[8,9] Low-pressure plasma pretreatments leave the bulk of the fibers intact and only modify the upper surface layers from 1 to 20 nm.[10] Besides, plasma polymerization is an emerging plasma process which is increasingly being used for the fabrication of functional coatings and has immense potential for future industrial applications.[11] Using this method, thin films can be produced easily with (i) a high control over the physical and chemical properties and (ii) a strong adhesion with most of the substrates. Furthermore, the combination of inorganic nanoparticles and plasma polymer network leads to the generation of new composite materials with unique properties.[12,13] Silver nanoparticles can be stabilized into plasma polymer thin films by using different approaches. For example, it is possible to combine plasma polymerization and silver particle deposition using sputtering from a silver target[14–17] or metal evaporation.[18] However, these approaches suffer from disadvantages as they need complex systems and involve many heavy and costly steps. An alternative strategy was recently reported by Vasilev et al.[12] and later by our group[19] in which an amine-containing or an acid-containing plasma polymer matrix interacts with silver ions (Ag^+) to generate electrovalent bonding, leading to Ag^+ loading of the plasma polymer. The silver ions were then reduced to silver using a reducing agent ($NaBH_4$) and the Ag atoms coalesced into nanoparticles. More recently, Kamar et al.[20] used this approach to load silver nanoparticles onto a polyethylene terephthalate (PET) mesh. Depending on the aforementioned studies, the amount of loaded AgNPs was controlled by playing with Ag^+ loading time, time of reduction,

Additional Supporting Information may be found in the online version of this article.

thickness of the plasma polymer layer or power used during plasma polymerization. Surprisingly, plasma duty cycle was never taken into consideration while it affects directly (i) the degree of crosslinking of the plasma polymer layer and (ii) the final concentration of anhydride groups contained in the plasma polymer layer, which both impact the AgNPs loading step. In this study, maleic anhydride was plasma-polymerized and subsequently hydrolyzed to lead to a carboxylic functionalized plasma polymer. Adjusting duty cycle during plasma polymerization allowed tailoring the number of carboxylic groups in the final plasma polymer layer and thus, the amount of loaded AgNPs onto the cotton fibers. The antibacterial activities were qualitatively measured against Gram-negative bacteria (*Escherichia coli*) and the durability of such coatings was tested during washing cycles.

EXPERIMENTAL

Materials

A cotton textile was purchased from Institut Français du Textiles et de l'Habillement (IFTH, Mulhouse, France). Briquettes of maleic anhydride (99.5% purity) were provided by Prolabo and were used as received. $AgNO_3$ (0.1*N*) and $NaBH_4$ (98% purity) solutions and briquettes of Phosphate buffered saline (PBS) were purchased from Sigma-Aldrich and were used as received.

Substrate Functionalization by Plasma Polymerization

The cotton sheets were cut into rectangular pieces and were treated by plasma polymerization as follows. Maleic anhydride was ground into a fine powder and loaded into a stoppered glass gas delivery tube. Plasma processing was carried out in a home-built RF plasma reactor (see Supporting Information Figure 1S). The plasma chamber consists of a glass tube (6 cm in diameter, 680 cm^3 in volume) coupled with an externally wound copper coil (4 mm diameter, 5 turns) and surmounted by a 20 cm round cylinder glass hall equipped with a "roll-to-roll" system. The chamber was fitted with a gas inlet, a Pirani pressure gauge, a two-stage rotary pump (Edwards) connected to a liquid nitrogen cold trap. An L-C matching network (Dressler, VM 1500 W-ICP) was used to match the output impedance of a 13.56 MHz r.f. power supply (Dressler, Cesar 133) to the partially ionized gas loaded by minimizing the standing wave ratio of the transmitted power. During electrical pulsing, the pulse shape was monitored with an oscilloscope. The average power $<P>$ delivered to the system was calculated using the following expression: $<P> = P_p\ [t_{on}/(t_{on} + t_{off})]$, where P_p is the average continuous wave power output and $t_{on}/(t_{on} + t_{off})$ is defined as the duty cycle (t_{on} is the "on" duration and t_{off} is the "off" duration during a single cycle). Prior to each experiment, the reactor was cleaned by scrubbing with detergent, rinsing in propan-2-ol, oven drying, followed by a 30 min high-power (60 W) air plasma treatment. The system was then vented to air and a cotton sheet was placed at 17 cm from the first copper coil followed by evacuation back down to base pressure. Subsequently, maleic anhydride vapor was introduced into the reaction chamber at a constant pressure of 0.2 mbar and with a flow rate of approximately 1.610^{-9} kg s^{-1}. At this stage, the plasma was ignited. The peak power delivered from the generator was 30 W (P_p) and the reflected power (P_r) was systematically estimated to 0 W. The frequency of the pulses was kept to 816 Hz and the DC was fixed to 2, 50, or 100%. The plasma was run for 2% of DC 30 min, 50% of DC during 8 min and 100% of DC (continuous wave) during 4 min. The different deposition times were judiciously selected to obtain the same thickness (≈30 nm) in all conditions. Upon completion of deposition, the r.f. generator was switched off and the monomer feed allowed to continue to flow through the system for a further 2-min period prior to evacuate back down to atmospheric pressure.

AgNPs Loading

Plasma polymer functionalized cottons were hydrolyzed by immersing the freshly modified cotton substrates in deionized water (pH = 6) for 24 h in order to convert the anhydride groups into carboxylic acid groups. Then, the containing carboxylic plasma polymer substrates were soaked in an aqueous solution of $AgNO_3$ (50 ppm) during 2 h in order to attach silver ions by ionic interactions. The silver nanoparticles (AgNPs) were subsequently reduced by soaking the substrate in a 1.10^{-3} g mL^{-1} aqueous solution of $NaBH_4$ during 1 h at room temperature. Finally, the cotton fibers loaded with AgNPs were

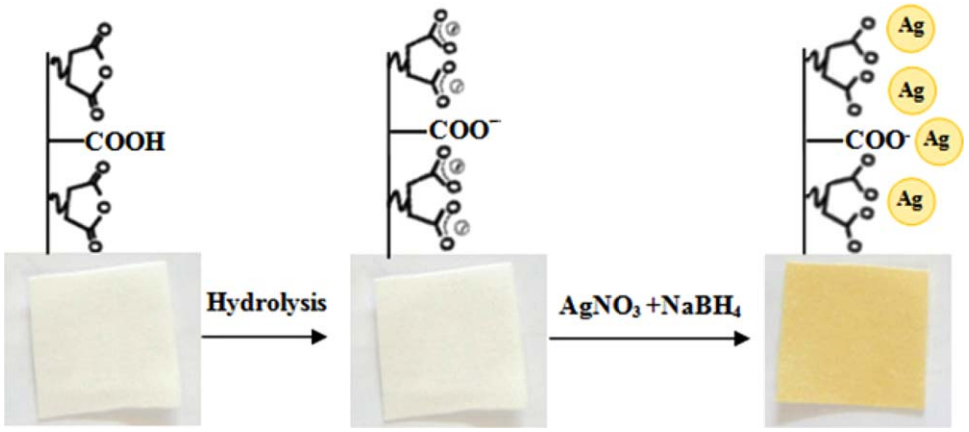

Figure 1. Synthesis scheme of the loading of AMpp-coated cotton fibers with AgNPs. [Color figure can be viewed in the online issue, which is available at wileyonlinelibrary.com.]

Table I. XPS Elemental Compositions of Native Cotton and MApp-Treated Cotton

Sample	%C	%O	O/C
Untreated cotton	67	33	0.49
MApp-treated cotton	74	26	0.35

washed with deionized water for several times and dried. The yellow color appeared on the samples due to the presence of AgNPs, as shown in Figure 1.

Characterization Techniques

UV–Visible Spectroscopy. UV–Visible spectroscopy measurements were carried out using a Lambda 750 (Perkin Elmer) rapid scan spectrometer equipped with two Hamamatsu R 955 photomultipliers. The light sources were deuterium (DL) and tungsten-halogen (THL) lamps (12 V), working in the range of 190–3300 nm. Spectra were the result of the sum of 100 scans. Windows-based Perkin Elmer UV Winlab software was used for data acquisition and analysis. Before each experiment, background was carried out without sample.

Scanning Electronic Microscopy Analysis. Scanning Electron Microscopy (SEM) observations were performed by using a FEI environmental microscope (Quanta 400 model) working at 30 keV. The films were observed using high vacuum mode.

Transmission Electron Microscopy. Transmission electron microscope (TEM) images were collected on a CM200 microscope (Philips) equipped with a LaB6 filament. The accelerating voltage was 200 kV. Samples were prepared by depositing several drops of a diluted AgNPs solution onto Cu grids coated with a thin holey carbon film.

Atomic Force Microscopy. AFM images were realized with a Dimension 3000 scanning probe microscope (Digital Instrument). A silicon cantilever was used for all measurements. The spring constant of the cantilever was 20–100 N/m. Typically, the surface morphology of 2 μm $\times$ 2 μm area near the center of each sample was observed by using the tapping mode of the scanning probe microscope.

Attenuated Total Reflection Fourier Transform Infrared. Attenuated Total Reflection Fourier Transform Infrared (ATR-FTIR) spectra were recorded with a Bruker IFS 66 FTIR spectrometer equipped with an ATR accessory from Specac. The spectrometer was equipped with a nitrogen cooled MCT detector. Spectra were the result of the sum of 256 scans and were recorded in the range of 4000–650 cm^{-1} with a spectral resolution of 4 cm^{-1}. A single reflection Ge crystal (refractive index ~4.0) with 65° beam incidence was used. The spectrum of a freshly cleaned Ge crystal was used as the background.

X-ray Photoelectron Spectroscopy (XPS). XPS spectra were recorded with a VG SCIENTA SES-200 spectrometer equipped with a concentric hemispherical analyzer. The incident radiation used was generated by a monochromatic Al Ka X-ray source (1486.6 eV) operating at 420W (14 kV; 30 mA). Photo-emitted electrons were collected at a take-off angle of 90° from the substrate, with electron detection in the constant analyzer energy mode. Survey spectra signal were recorded with a pass energy of 500 eV while high resolution spectra were recorded with a pass energy of 100 eV. Peak fitting was carried out with mixed Gaussian–Lorentzian (30%) components with equal full-width-athalf-maximum (FWHM) using CASAXPS software. The binding energy of the CH_x component in the C1s region was set to 285.0 eV and used for referencing. The surface composition expressed in at.% was determined using integrated peak areas of each components and take into account transmission factor of the spectrometer, mean free path and Scofield sensitivity factors of each atom (C1s: 1.00, O1s: 2.93).

Bacterial Strain and Culture

Experiments were conducted with the Gram-negative *Escherichia coli* (*E. coli*) PHL628 (MG1655).[21] One microliter of bacteria stock culture (stored at −80°C) were used to inoculate 10 mL of selective growth medium (M63G[21]; pH 6.8), resulting in a preculture that was further grown overnight at 30°C. This culture was used to inoculate a second preculture (10 vol % of the last preculture) which was grown for 4 h in the same conditions.

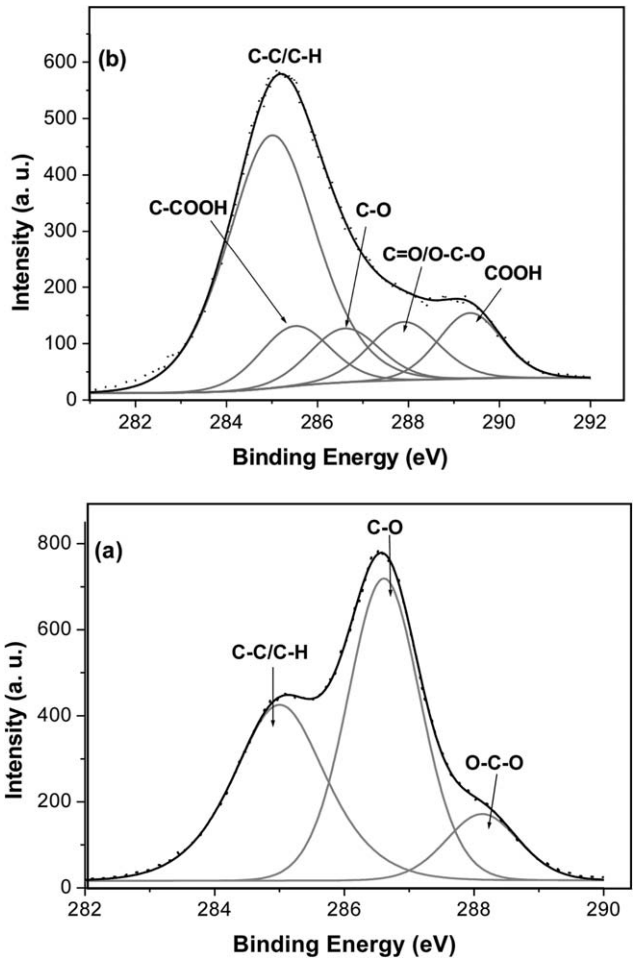

Figure 2. C1s XPS core-level spectra of (a) native cotton and (b) MApp-treated cotton.

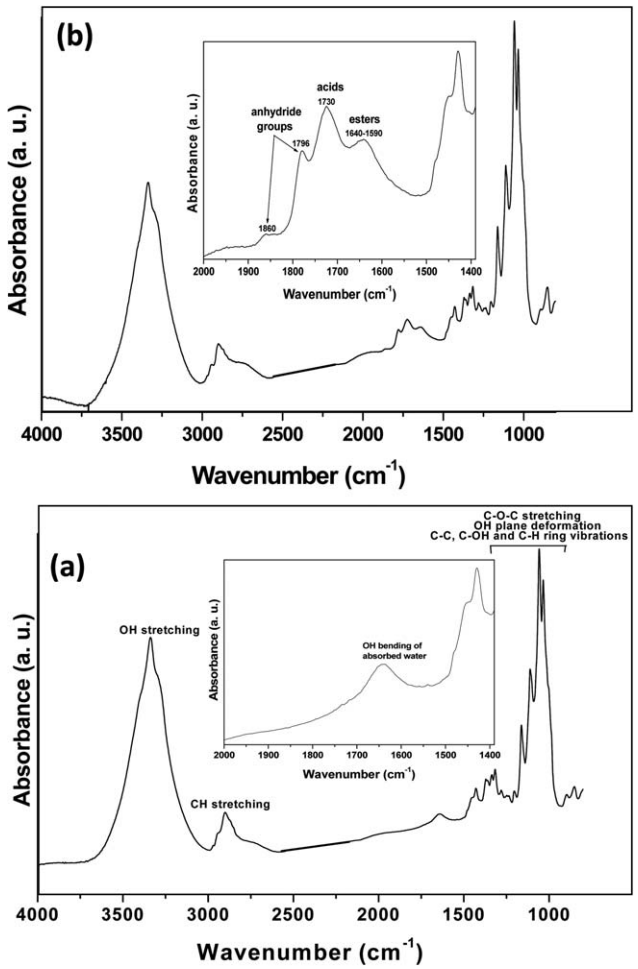

Figure 3. Infrared spectra of (a) native cotton and (b) MApp-treated cotton. Insets are their spectra between 1400 and 2000 cm^{-1}. The CO_2 absorbance band between 2500 cm^{-1} to 2225 cm^{-1} was eliminated by an atmosphere correction function.

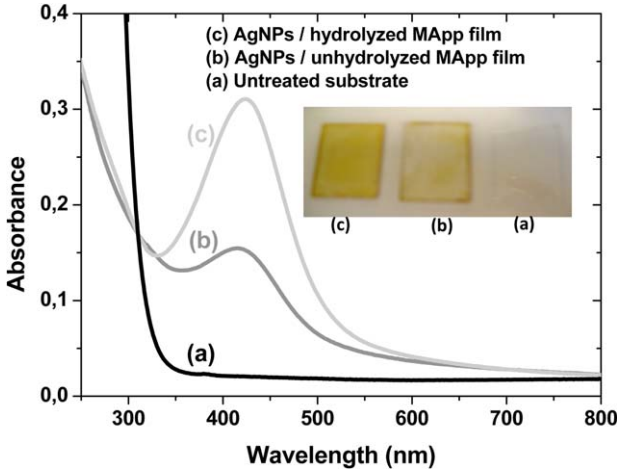

Figure 4. UV–Visible absorbance spectra of glass substrates after deposition of AgNPs: (a) untreated, (b) unhydrolyzed MApp, and (c) hydrolyzed MApp-treated glass slides (insets are the digital images under indoor light). [Color figure can be viewed in the online issue, which is available at wileyonlinelibrary.com.]

Antibacterial Assays

Before antibacterial tests, samples were sterilized by exposing them to UV radiation (257 nm) at 2.5 cm from UV lamp during 10 min.

Agar-Plate Diffusion Test. Totally, 100 μL of the fresh second pre-culture bacterial suspension was spread on Luria-Bertani (LB) agar-supplemented growth medium (15%w.) in order to form a thin bacterial film. The sterilized material samples were placed in contact with the previously homogenously inoculated agar plate (top side of the samples in contact with agar). After overnight incubation at 30°C, bacterial growth around the samples was observed in order to identify the potential presence of zones without bacterial growth (growth inhibition area).

Inhibition Test on Planktonic Bacteria. Sterilized material samples were placed in 35 mm diameter Petri dishes and inoculated with 4 mL of the fresh second preculture. After 2 h of incubation at 30°C, 3 mL of bacterial suspension was removed and replaced by 3 mL of NaCl 9 g/L solution (samples were not exposed to air during this stage). This washing procedure was repeated three times. The initial supernatant and removed washing solutions were kept for bacterial concentration analysis by measuring optical density (OD) at 630 nm.

Inhibition Test on Adhered Bacteria. Bacteria were stained with 1 µL/mL Syto® 9 fluorescence dye (Molecular Probes, 5 m*M*) added to the last washing NaCl solution. Adhered bacteria were observed directly in the last washing solution under an epifluorescence microscope (Upright Olympus Bx51) equipped with a long working-distance objective. Microscopic images were analyzed using ImageJ software.[22]

Statistical Relevance. Five places were analyzed on each sample. Two samples of each condition were analyzed for each experiment. Experiments were repeated two times. Statistical significations were tested by a standard Student-test.

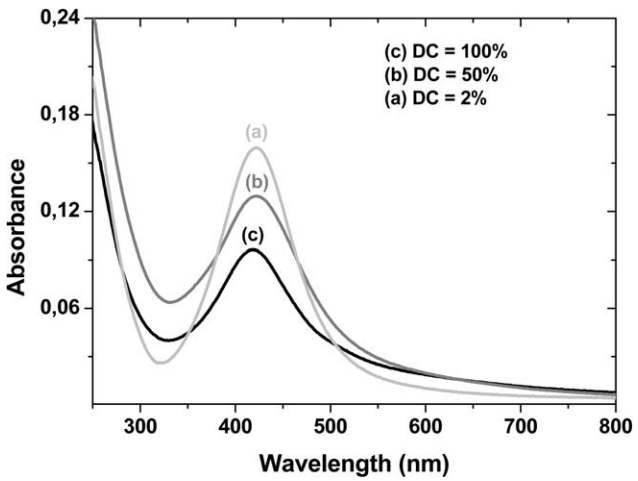

Figure 5. Effect of plasma duty cycle (DC) on UV–Visible absorbance of hydrolyzed MApp-treated glass substrates after deposition of AgNPs. Deposition times have been chosen in order to keep the thickness of the plasma polymer layer constant and equal to (30 ± 5) nm.

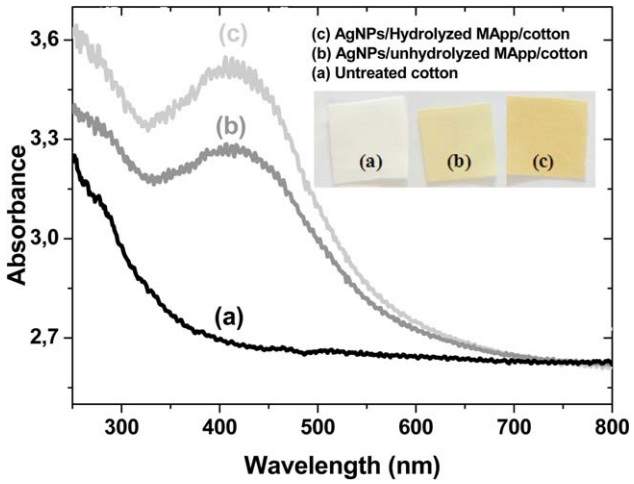

Figure 6. UV–Visible absorbance spectra of cotton substrates after deposition of AgNPs: (a) untreated, (b) unhydrolyzed MApp, and (c) hydrolyzed MApp-treated cotton (insets are their digital images under indoor light). [Color figure can be viewed in the online issue, which is available at wileyonlinelibrary.com.]

RESULTS AND DISCUSSION

In this study, a solvent free-dry-plasma polymerization process was employed to functionalize textile fabrics for anchoring AgNPs in order to achieve antibacterial property. Plasma functionalized textile surfaces were obtained by depositing a maleic anhydride plasma polymer thin film (MApp) onto cotton substrates. All anhydride groups were subsequently converted into carboxylic acid groups ($pK_a < 5$) by hydrolysis.[19,23] These charged groups were expected to allow attaching silver ions on the surface by favorable electrostatic interactions. Afterwards, these ions were reduced into silver nanoparticles.

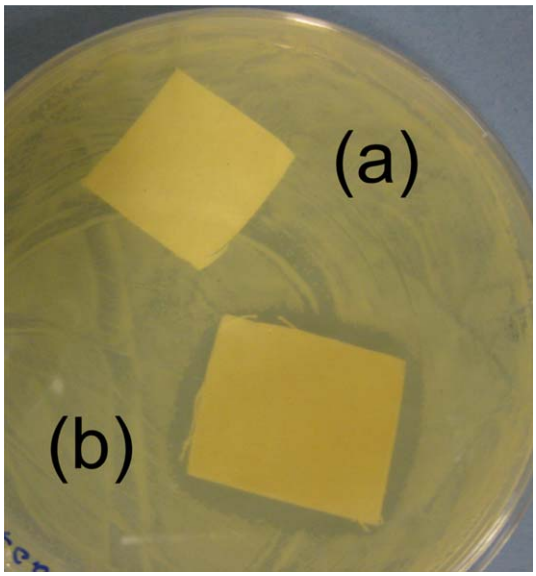

Figure 7. Bacterial growth on nutritive agar plates in the surroundings of: (a) native cotton and (b) AgNPs-treated cotton. [Color figure can be viewed in the online issue, which is available at wileyonlinelibrary.com.]

Maleic Anhydride Plasma Polymer Functionalized Cotton

Characterizations of MA plasma polymer functionalized cotton were performed only on the substrates exposed to a 2% of duty cycle. Changes in plasma polymer properties according to the duty cycle used are already well known.[24] XPS was performed to determine the changes in the surface composition of the cotton after plasma treatment. XPS survey spectrum of native cotton present only two peaks at 285 eV and 533 eV, which are assigned to C1s and O1s respectively (see Supporting Information Figure 2S). This spectrum is coherent with the chemical structure of cellulose. The carbon peak is narrow and well defined while the plasma treatment extends the C1s peak to higher binding energies; the C1s peak is then centered at ~287 eV. A preliminary quantitative analysis reveals a decrease in the O/C atomic ratio from 0.49 before plasma treatment to 0.35 after plasma treatment (Table I). Even if it is well established that XPS analysis cannot give a full account of the chemical composition (quantitative analysis) for cotton textile samples due to their rough surface,[25] we have tried to examine the decomposition of C1s XPS peak. The C1s peak decomposition of native cotton [Figure 2(a)] reveals three major components at 285, 286.6, and 288.1 eV assigned to C—C/C—H (hydrocarbon), C—O and O—C—O bonds, respectively.[25,26] Figure 2(b) showed the C1s peak decomposition of hydrolyzed MApp-treated surface revealing five major components assigned to five types of carbon functionality: hydrocarbon (CHx/C—C) at 285.0 eV), carbon in alpha position of carboxylic acid groups (C—COOH) at 285.5 eV, carbon singly bonded to oxygen (—C—O) at 286.6 eV, carbon doubly bonded to oxygen (O—C—O/—C=O at 287.9 eV), and carboxylic groups (COOH) at 289.4 eV.[27,28] The presence of carboxylic groups results in a ring opining of the cyclic anhydride in the near surface region of the plasma polymer after hydrolysis.

The chemical fingerprints of cotton sheet before and after plasma treatment have been also studied using ATR-FTIR analysis (Figure 3). The spectrum of native cotton [Figure 3(a)] exhibits strong absorption bands in the region of 1000–1200 cm^{-1} corresponding to C—O—C stretching, OH plane deformation and C—C, C—OH, and C—H ring and side group vibrations. Other infrared bands in the region of 1250–1450 cm^{-1} belong to HCH, OCH, or CH bending and CH_2 rocking vibrations. The presence of absorbed water is evident from the strong absorbance at 1624 cm^{-1} belonging to OH bending. Other strong absorption bands have been observed around 3300 cm^{-1} and 2800–3000 cm^{-1} corresponding to O—H stretching and C—H symmetrical stretching absorption, respectively. These characteristic infrared absorbances are consistent with those of the typical cellulous backbone.[29,30] After deposition of maleic anhydride plasma polymer and hydrolysis, the ATR-FTIR spectrum [Figure 3(b)] shows new absorption bonds corresponding to carboxylic and ester groups around 1730 cm^{-1} and 1590−1640 cm^{-1}, respectively. The presence of these infrared bands confirms that the hydrolysis reaction of MApp is well performed.

XPS and FTIR studies have shown the cotton fabric was conformally coated with a thin polymer film, poly(maleic anhydride) via plasma polymerization. The XPS analysis did not show the

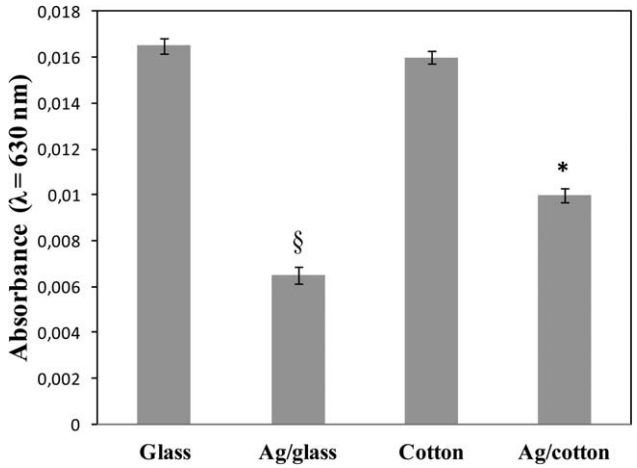

Figure 8. Optical absorbance at 630 nm of bacterial suspension culture (*: significantly different from cotton [$P > 95\%$); §: significantly different from glass ($P > 95\%$)].

presence of anhydride group in the accompanying high-resolution C1s envelope. However, the background of maleic anhydride pulsed plasma polymer infrared bands (asymmetric C═O stretching at 1860 cm^{-1} and symmetric C═O stretching at 1796 cm^{-1} [31,32]) were observed. These observations can be due to the difference between the analyzed depth of XPS and ATR-FTIR analyses. The XPS technique is extremely sensitive to the surface state (5−10 nm), whereas the analyzed depth for ATR-FTIR technique is varied between few nanometers to a few micrometers as a function of wavelength. This confirms that hydrolysis reaction has only occurred at the solid-solution interface (in the near surface region of the plasma polymer).

Changes in cotton fibers morphology were examined by SEM (see Supporting Information Figure 3S). The as-received cotton sample has a tightly woven, fibrous structure. No change in the morphology was observed when the cotton sample was modified by MApp. The plasma polymerization process allows extremely conformal coating and preserves the surface morphology of the textile. As a result, the pores of porous fabrics remain undamaged as shown by SEM images. Moreover, it is easy to coat both sides of a porous substrate since the coating material can easily penetrate through the pores of the porous substrate. Hence, both sides of textile will be functionalized at the same time and thus enhance the loading of Ag on the fabrics.

Characterization of AgNPs Loaded onto Plasma Polymer Layer

In order to better characterize the AgNPs after loading, the plasma polymer layer was first deposited (2% of duty cycle, 30 min) onto "model" surfaces (i.e. glass slides or MET grids). Ag cations were loaded by simply dipping of MApp functionalized textile in aqueous solution of $AgNO_3$. Subsequently, AgNPs were easily obtained in one-step manner based on the reaction between $AgNO_3$ and $NaBH_4$. TEM images of the AgNPs showed a narrow size distribution without undesired aggregation (see Supporting Information Figure 4S). The average size of AgNPs is about 8 nm with broad size distribution, ranging from 3 nm to 34 nm. AgNPs exhibited a spherical shape. After soaking of substrates in $NaBH_4$ solution, the nanoparticles were homogeneously well dispersed on the surface of plasma polymer as confirmed by AFM (see Supporting Information Figure 5S). The average size (∼15 nm) and polydispersity determined by AFM are in accordance with the results observed in TEM images.

The loading of silver was also verified by presence a characteristic surface plasmon resonance (SPR) band of AgNPs in UV–Vis spectra of the sample, which can confirm the formation of crystalline spherical AgNPs.[33] The SPR band arises from the coherent existence of free electrons in the conduction band due to the small metal particle size.[33]

Figure 4-spectrum (c) shows the UV–Visible absorbance spectra of plasma polymer-treated glass slides after incorporation of AgNPs. The glass slides exhibit a strong absorption peak with a maximum at 415 nm (FWHM = 96 nm) and present light yellow. This phenomenon is due to the surface Plasmon absorption of AgNPs, which can confirm the formation of crystalline spherical AgNPs.[33] As control, both spectra of unhydrolyzed MApp film and hydrolyzed MApp film without loading of AgNPs were investigated. The corresponding spectra were overlapped with the spectrum obtained in the case of the untreated glass slides [spectrum (a) in Figure 4]. In both cases, the samples exhibit transparency and no color. Any Plasmon resonance band was detected due to the absence of AgNPs. Similar results

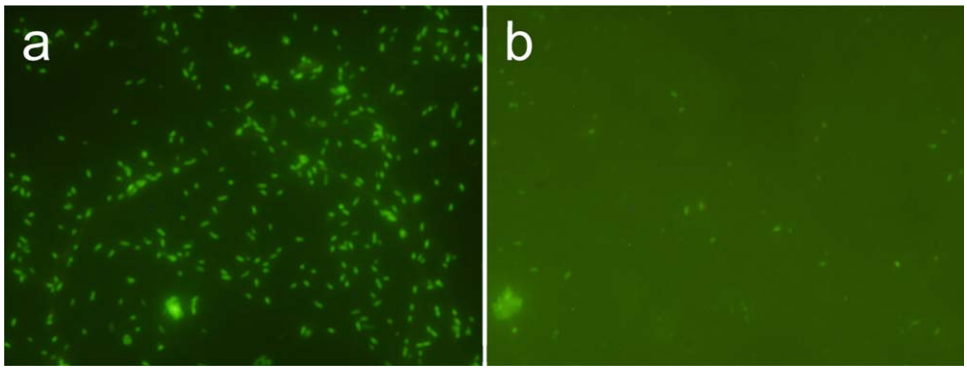

Figure 9. Epifluorescence microscopic images of biofilms on (a) untreated glass, (b) AgNPs-treated galss. [Color figure can be viewed in the online issue, which is available at wileyonlinelibrary.com.]

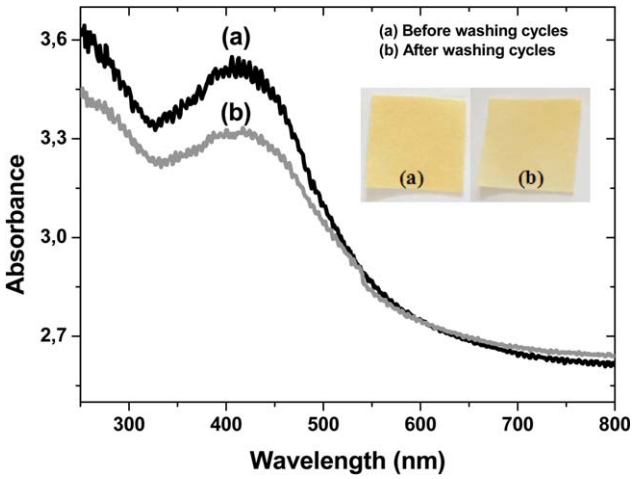

Figure 10. UV–Visible absorbance spectrum of AgNPs-loaded cotton (a) before and (b) after washing cycles (insets are their digital image under indoor light). [Color figure can be viewed in the online issue, which is available at wileyonlinelibrary.com.]

were obtained in the case of the hydrolyzed MApp film after treatment with silver ions but before reduction. However, a Plasmon resonance band was obtained in the case of the unhydrolyzed MApp film with silver ions and after reduction [spectrum (b) in Figure 4]. This band showed a low intensity because of the small quantity of silver ions attached onto the MApp film. This result confirms the presence of carboxylic acid groups in the plasma polymer matrix before hydrolysis.[27,31,34,35] Hydrolyzed plasma polymer on cotton fabric has anionic COO^- groups at pH above 4.5 that help in two ways in synthesis of embedded AgNPs: (i) anionic COO^- groups interact with Ag^+ ions through ionic interactions and thus enhance the loading of Ag on the MApp-treated cotton, (ii) it is possible that poly(maleic anhydride) chains act as a stabilizer and entrap the AgNPs and restrict the formation of silver aggregates.

All aforementioned results demonstrate that the carboxylic acid groups play an important role in the loading of AgNPs on the surface by immobilizing silver ions. The concentration of acid groups available to interact with silver ions strongly depends on the initial concentration of anhydride groups in the plasma polymer. A general consensus in the maleic anhydride plasma polymerization literature is that the reactivity of the anhydride groups is strongly dependent on duty cycle $t_{on}/(t_{on} + t_{off})$ ratio, and differences in chemical properties are evident even when deposition is carried out under same nominal power P_{nom} (i.e., $P_{nom} = P_p[t_{on}/(t_{on} + t_{off})]$).[24,36,37] Changes in the duty cycle lead to significant changes in monomer fragmentation which influences significantly the final atomic composition of the plasma polymer layers. An increase in the duty cycle leads to an increase of fragmentations of the precursor molecule.[27,31] Consequently, different reaction mechanisms occur and subsequently less anhydride functionalities are retained in the plasma polymer thin film structure.[27,35] Figure 5 shows the effect of plasma duty cycle (DC) on the absorbance of hydrolyzed MApp-treated substrates after loading of AgNPs. The maleic anhydride plasma polymer was deposited using a peak power (Pp) of 30W and different $t_{on}/(t_{on} + t_{off})$ ratio, 2%]Figure 5—spectrum (a)], 50% [Figure 5 spectrum (b)], and 100% [Figure 5 spectrum (c)], respectively. Deposition times have been chosen in order to keep the thickness of the plasma polymer layer constant and equal to (30 ± 5) nm. The UV–Visible absorbance spectra of AgNPs depicted peak maxima in the range from 410 to 425 nm with respective decrease in optical density by varying duty cycle from 2 to 100%. These results demonstrate that the loaded AgNPs quantity decrease with increasing the plasma duty cycle. In other words, a lower concentration of anhydride groups was expected in the case of high duty cycle leading to a lower concentration of acid groups after hydrolysis. Therefore, the plasma duty cycle of 2% is optimal for loading a maximum of AgNPs onto the surface.

Even if those measurements were performed on a glass slides, we expected the results to remain valid on a cotton substrate that was chemically modified in the same way (i.e., plasma polymer functionalized). For example, Figure 6 shows the UV–Visible absorbance spectra after loading of AgNPs of untreated and plasma polymer-treated cotton fabrics with optimal conditions. The same results can be observed: only the unhydrolyzed and hydrolyzed MApp-treated cotton show yellow light and exhibit a SPR peak with a maximum at 410−415 nm.

Evaluation of Antimicrobial Properties

Antibacterial activity of plasma-treated cotton using optimal conditions was determined in terms of inhibition zone formed on agar medium and inhibition of growth of planktonic and adhered bacteria. With the diffusion test on agar medium, the native cotton did not show any antibacterial activity (bacterial growth was seen on the agar surface as indicated by the presence of colonies) [Figure 7(a)]. In this case, bacterial growth was observed under and within cotton samples. In contrast, AgNPs modified cotton textiles placed on the bacteria-inoculated agar surfaces led to inhibit growth of all the bacteria under and around them. Distinct zones of inhibition (clear areas with no bacterial growth) were observed around the cotton samples for *E.coli* (41 ± 4% of the sample surface) [Figure 7(b)], whilst high bacterial growth as indicated by bacterial growth lawn was observed everywhere. Also, no bacterial growth was observed under or within AgNPs-modified cotton. The zone of inhibition is the result of the expected leaching of active biocidal species (Ag^+ ions) from the embedded Ag particles present in the fabric into the surrounding aqueous medium.[38] The plasma MA polymer acts as a reservoir for the out-diffusion of Ag ions which diffuse out of the polymer.

Figure 8 shows the optical absorbance at 630 nm of bacterial suspension culture after 2 h of incubation in the presence of different samples (untreated or treated with AgNPs). Absorbance measurements show usual growth of planktonic bacterial in the absence of AgNPs (untreated glass and cotton). In contrast, in the presence of samples coated with AgNPs, the absorbance is significantly lower than with untreated sample, indicating a toxic effect of Ag^+ released into the culture medium.

Epifluorescence studies [Figure 9(a,b)] showed that AgNPs-treated substrates were less colonized by bacteria than untreated

sample. The biofilm quantity was significantly reduced on AgNPs/glass samples due to the presence of Ag antibacterial species. The results of epifluorescence microscopic studies were in good agreement with the inhibition test on planktonic bacteria. The quantity of adhered bacteria was determined on glass only, since untreated cotton is auto-fluorescent. This auto-fluorescence signal was significantly higher than the signal measured from the stained bacteria, preventing to distinguish them from the substrate.

Durability of the Antibacterial Coating

To find out how strongly the silver particles are attached to the textile surface, AgNPs-modified cotton were subjected to three washing cycles in heated water bath (40°C) with active tension agents for 30 min under stirring. After drying, the cotton sheets kept their original color (yellow), indicating that the silver particles are quite strongly linked to the cotton textile surface. UV–Visible analysis showed no obvious change of the absorbance spectra of the cotton (Figure 10). Indeed, the plasmon resonance band appeared and sample retains its yellow color attesting the presence of AgNPs on the surface after washing. We also expect any significant change in its antibacterial effect after washing.

The method presented here is advantageous in that (i) the conformal coating of textile substrates via a solvent free-dry process (plasma polymerization) allows for the use of various substrate materials and (ii) the tailoring the amount of loaded AgNPs can be easily and simply achieved by varying plasma duty cycle for plasma polymer deposition. Therefore, further investigations are under progress to quantify antibacterial effect in function of the loaded AgNPs characteristics (loaded quantity and particle size). This will allow to adapt AgNPs quantity and AgNPs size in the final coating in agreement with the necessity of the clinical applications.

CONCLUSIONS

In a context of "green chemistry" we have shown that plasma polymers can be easily used for loading silver nanoparticles onto the surface of cotton textiles. The fibers were functionalized with anhydride groups that were subsequently converted into carboxylic acid groups by hydrolysis. The silver ions Ag^+ were then adsorbed via carboxylic acid groups at ambient temperature and AgNPs can be generated and distributed homogeneously on the surface of plasma modified cotton by simply adding $NaBH_4$ reducing agent. The size of the AgNPs ranged from 5 nm to 34 nm with average size at about 8 nm. Interestingly, changing the duty cycle value during plasma polymer deposition can vary the amount of loaded AgNPs. The higher loaded AgNPs quantity was obtained with low duty cycle values. The plasma-modified cotton with AgNPs showed significant antibacterial activity.

REFERENCES

1. Ripoll, L.; Bordes, C.; Marote, P.; Etheve, S.; Elaissari, A.; Fessi, H. *Colloids Surf. Part: A Physicochem. Eng. Aspects* **2012**, *397*, 24.
2. Leelajariyakul, S.; Noguchi, H.; Kiatkamjornwong, S. *Prog. Org. Coat.* **2008**, *62*, 145.
3. Sarier, N.; Onder, E. *Thermochim. Acta* **2012**, *540*, 7.
4. Akhavan, O.; Ghaderi, E. *Curr. Appl. Phys.* **2009**, *9*, 1381.
5. Morones, J. R.; Elechiguerra, J. L.; Camacho, A.; Holt, K.; Kouri, J. B.; Ramirez, J. T.; Yacaman, M. *J. Nanotechnology* **2005**, *16*, 2346.
6. Akhavan, O.; Abdolahad, M.; Asadi, R. *J. Phys. Part D: Appl. Phys.* **2009**, *42*, 135416-1.
7. Akhavan O. *J. Colloid Interface Sci.* **2009**, *336*, 117.
8. Bozzi, A.; Yuranova, T.; Kiwi, J. *J. Photochem. Photobiol. Part: A Chem.* **2005**, *172*, 27.
9. Yuranova, T.; Rincon, A. G.; Bozzi, A.; Parra, S.; Pulgarin, C.; Albers, P.; Kiwi, J. *J. Photochem. Photobiol. Part: A Chem.* **2003**, *16*, 27.
10. Kinloch, A. Adhesion and Adhesives; Chapman and Hall: New York, **1998**. 83 p.
11. Grill, A. Cold Plasmas in Materials Fabrication. IEEE Press; New York, **1994**. 272 p.
12. Vasilev, K.; Sah, V.; Anselme, K.; Ndi, C.; Mateescu, M.; Dollmann, B.; Martinek, P.; Ys, H.; Ploux, L.; Griesser, H. *J. Nano. Lett.* **2010**, *10*, 202.
13. Kulaga, E.; Ploux, L.; Balan, L.; Schrodj, G.; Roucoules, V. *Plasma Process. Polym.* **2014**, *11*, 63.
14. Körner, E.; Aguire, M. H.; Fortunato, G.; Ritter, A.; Rühe, J.; Hegemann, D. *Plasma Process. Polym.* **2010**, *7*, 619.
15. d'Agostino, R. *J. Photopolym. Sci. Technol.* **2005**, *18*, 245.
16. Sardella, E.; Favia, P.; Gristina, R.; Nardulli, M.; d'Agostino, R. *Plasma Process. Polym.* **2006**, *3*, 456.
17. Favia, P.; Vulpio, M.; Marino, R.; d'Agostino, R.; Mota, R. P.; Catalano, M. *Plasmas Polym.* **2000**, *5*, 1.
18. Heilmann, A.; Werner, J. *Thin Solid Films* **1998**, *317*, 21.
19. Airoudj, A.; Ploux, L.; Kulaga, E.; Roucoules, V. *Adv. Eng. Mater.* **2010**, *13*, B360.
20. Kumar, V.; Jolivalt, C.; Pulpytel, J.; Jafari, R.; Arefi-Khonsari, F. *J. Biomed. Mater. Res. Part: A* **2013**, *101*, 1121.
21. Vidal, O.; Longin, R.; Prigent-Combaret, C.; Dorel, C.; Hooreman, M.; Lejeune, P. J. *J. Bacteriol.* **1998**, *180*, 2442.
22. Rasband, W. S. Image J, U.S. National Institutes of Health, Bethesda, MD **1997**.
23. Geissler, A.; Vallat, M.-F.; Fioux, P.; Thomann, J. S.; Frisch, B.; Voegel, J. C.; Hemmerle, J.; Schaaf, P.; Roucoules, V. *Plasma Process. Polym.* **2010**, *7*, 64.
24. Airoudj, A.; Schrodj, G.; Vallat, M.-F.; Fioux, P.; Roucoules, V. *Int. J. Adhes. Adhes.* **2011**, *31*, 498.
25. Kontturi, E.; Thüne, P. C.; Niemantsverdriel, J. W. *Langmuir* **2003**, *19*, 5735.
26. Gaiolas, C.; Costa, A. P.; Silva, M. S.; Thielemans, W.; Amaral, M. E. *Ind. Crop. Prod.* **2013**, *43*, 114.
27. Ryan, M. E.; Hynes, A. M.; Badyal, J. P. S. *Chem. Mater.* **1996**, *8*, 37.

28. Beamson, G.; Briggs, D. High-Resolution XPS of Organic Polymers, The Scienta SCA 300 Database, Wiley; New York, **1992**. 26 p.
29. Zhang, C. D.; Price, L. M.; Daly, W. H. *Biomacromolecules* **2006**, *7*, 139.
30. Kemp, W. Organic Spectroscopy; Macmillan Education: Hampshire, **1987**; 393 p.
31. Siffer, F.; Ponche, A.; Fioux, P.; Schultz, J.; Roucoules, V. *Anal. Chim. Acta* **2005**, *539*, 289.
32. Schiller, M.; Kulish, W. *Surf. Coat. Technol.* **1998**, *98*, 1590.
33. Sun, Y. G.; Xia, Y. N. *Analyst* **2003**, *128*, 686.
34. Roucoules, V.; Siffer, F.; Ponche, A.; Egurrola, U.; Vallat, M.-F. *J. Adhesion* **2007**, *83*, 875.
35. Schiller, S.; Hu, J.; Jenkins, A. T. A.; Timmons R. B.; Sanchez-Estrada, F. S.; Knoll, W.; Förch, R. *Chem. Mater.* **2002**, *14*, 235.
36. Mishra, G.; McArthur, S. L. *Langmuir* **2010**, *26*, 9645.
37. Dirani, A.; Wieder, F.; Roucoules, V.; Airoudj, A.; Soppera, O. *Plasma Process. Polym.* **2010**, *7*, 571.
38. Wang, H.; Wang, J.; Hong, J.; Wei, Q.; Gao, W.; Zhu, Z. *J. Coat. Technol. Res.* **2007**, *4*, 101.